Reconstruction and fitting of second-harmonic signals by wavelength modulation spectroscopy method based on fast Fourier transform

Linquan Lai (赖林权)[1], Yue Chen (陈 玥)[1], Kongtao Chen (陈孔涛)[1], Jiale Tang (唐嘉乐)[1], Kaiwen Yin (尹楷文)[1], Fuqiang Jia (贾富强)[1*], Dun Qiao (乔 盾)[2], Yuanlong Fan (范元龙)[2], Kang Li (李 康)[2], and Nigel Copner[2]

[1] Fujian Key Laboratory of Ultrafast Laser Technology and Applications, School of Electronic Science and Technology, Xiamen University, Xiamen 361005, China

[2] Wireless & Optoelectronics Research & Innovation Centre, Faculty of Computing, Engineering & Science, University of South Wales, Wales CF37 1DL, UK

*Corresponding author: jiafq@xmu.edu.cn

Conventional wavelength modulation spectroscopy (WMS) is vulnerable to the influence of low-frequency noise. Accuracy of the method highly depends on the performance of the costly lock-in amplifier. In this article, we report a new and effective method for reconstructing second-harmonic signals through WMS based on fast Fourier transform (FFT). This method is less disturbed by low-frequency noise because it does not use a low-frequency ramp wave. Formulation and detection procedures were presented. The discrete second-harmonic waveform can be obtained by continuously changing the DC signal and FFT analysis in this method. Second-harmonic waveforms acquired by the two means are generally consistent. The experimental study validates the obtained gas concentration from 5% to 30%, showing a good linear relationship by the proposed method. The maximum relative error on concentration extraction is 2.87%; as for conventional WMS, this value is 4.50%. The developed measurement method may have potential in computed tomography.

Keywords: fast Fourier transform; wavelength modulation spectroscopy; second-harmonic waveform.
DOI: 10.3788/COL202220.093001

1. Introduction

The progress of laser and spectroscopy technology has greatly promoted the development of material detection technology[1,2]. Among them, tunable diode laser absorption spectroscopy (TDLAS) has been widely employed in gas detection across the energy, petrochemical, and mining industries because of its non-intrusiveness and high accuracy[3–8]. It is developed into two major approaches: direct absorption spectroscopy (DAS) and wavelength modulation spectroscopy (WMS). WMS has high sensitivity and signal-to-noise ratio (SNR) through harmonic detection. Numerous measurement results have shown that WMS is more sensitive by one to two orders of magnitude than DAS[9].

In 1981, Reid et al. proposed the expression of second harmonic by combining WMS and TDLAS provided in gas concentration measurements[10].

In WMS, the lock-in amplifier is usually used to extract each harmonic. The performance of the lock-in amplifier directly determines the accuracy of the measurement results. In addition, the initial phase difference between the signal to be measured and the reference signal will also affect the amplitude of the second harmonic.

Du and Peng proposed a calibration-free wavelength modulation DAS (WM-DAS) method in 2018, which only uses the sine wave to scan the gas absorption spectrum and recover the absolute absorbance profile of gas based on fast Fourier transform (FFT)[9]. However, since this approach is essentially DAS and is only suitable for weak absorption, and the modulation frequency is only 100 Hz, it is unable to efficiently reduce low-frequency noise interference. In 2020, Liu et al. proposed and used a method to directly obtain the whole second-harmonic waveform using FFT, but this method uses the ramp wave and sine wave to modulate the laser like WMS, which cannot obtain the second-harmonic peak in one step[11,12]. In 2021, Li proposed a natural logarithmic wavelength modulation spectrum, which is more suitable for the case of large absorbance[13].

Inspired by the above researches, in this paper, we propose a novel method to reconstruct and fit the second-harmonic waveform by WMS based on FFT (FFT-WMS). Conventional WMS modulates the laser by superimposing the sine wave with the

ramp wave and then extracts the second harmonic through the lock-in amplifier[9]. In FFT-WMS, the DC signal is superimposed with the sine wave to modulate the laser, and then the transmitted light intensity is analyzed by FFT for reconstruction and fitting of the second-harmonic signals. This method is less disturbed by low-frequency noise because it does not use low-frequency scanning signal.

2. Theory of WMS

In 1965, Arndt *et al.* deduced the analytical expression of the Lorentzian profile's Fourier series in the modulation spectrum and gave the mathematical expressions of the first harmonic and second harmonic with respect to modulation depth[14]. In 1981, Reid *et al.* combined WMS with TDLAS to give the second-harmonic expression in gas concentration measurement[10].

The transmitted light intensity $I_t(\nu)$ of an electromagnetic wave of optical frequency ν passing through path length L through absorbing gas is given by

$$I_t(\nu) = I_0 e^{-\alpha(\nu)\chi L}, \tag{1}$$

where $\alpha(\nu)$ is the profile function of the gas absorption line, and the gas concentration is denoted by the letter χ. The wavelength modulation is based on the low-frequency scanning current signal of the laser, and then a high frequency sine wave signal (modulation frequency is f) is added to realize wavelength

modulation. The instantaneous frequency $\nu(t)$ of the laser can be computed as follows:

$$\nu(t) = \nu_c + \alpha \cos(2\pi f t). \tag{2}$$

Here, ν_c is the frequency of laser corresponding to the scanning current signal, and α is the frequency modulation amplitude corresponding to the modulation signal.

In practice, tuning the modulation wavelength by the current will change the output power of the laser, so the intensity of the laser varies with the wavelength and can expressed as

$$I_0 = I_c + \Delta I \cos(\theta + \psi). \tag{3}$$

Among them, I_c is the average intensity of the output laser, ΔI is the amplitude of the light intensity modulation, and ψ is the phase difference between the wavelength modulation and the light intensity modulation. $\theta = 2\pi f t$, and the Fourier series were used to extend the transmitted light intensities:

$$I_t(\nu_c, \theta) = I_0 \sum_{n=0}^{\infty} H_n(\nu_c) \cos(n\theta). \tag{4}$$

The phase difference between frequency modulation and light intensity modulation can be eliminated by adjusting the phase in a lock-in amplifier circuit so that $\psi = 0$. The second harmonic used to derive the gas concentration can be expressed as

$$H_2'(\nu_c) = \frac{\Delta I}{2} H_1(\nu_c) + I_c H_2(\nu_c) + \frac{\Delta I}{2} H_3(\nu_c). \tag{5}$$

Due to the existence of light intensity modulation ΔI, both the first harmonic and the third harmonic will affect the second harmonic. This phenomenon is also called residual amplitude modulation (RAM). The size of the harmonic signal will decay rapidly with the increase of harmonic number. When the modulation amplitude is relatively small, we tend to ignored the RAM effect (that is, $\Delta I = 0$).

At normal temperature and pressure, the profile of the absorption spectrum satisfies the Lorentzian profile and can be expressed as

$$g_L(\nu) = \frac{1}{(\nu - \nu_0)^2 + \alpha^2}, \tag{6}$$

where γ is the half-width at half-maximum (HWHM) of the Lorentzian profile, and ν_0 is frequency of the line center.

Define two dimensionless parameters: $x = \frac{\nu_c - \nu_0}{\alpha}$, $m = \frac{\gamma}{\alpha}$.

The expression of the second harmonic can be transformed into

$$H_2(x, m) = \frac{L\chi}{\alpha^2} \left[\frac{4}{m^2} - \frac{\sqrt{2}(M + 1 - x^2)\sqrt{\sqrt{M^2 + 4x^2} + M} + 4x\sqrt{\sqrt{M^2 + 4x^2} - M}}{m^2\sqrt{M^2 + 4x^2}} \right], \tag{7}$$

where $M = 1 + x^2 + m^2$. At the center of the absorption line $x = 0$, the peak value P_{2f} of the second harmonic can be extracted from the lock-in amplifier:

$$P_{2f} \propto \frac{I_0 CL}{\alpha^2} \left\{ \frac{2}{m^2} \left[2 - \frac{2 + m^2}{(1 + m^2)^{1/2}} \right] \right\}. \tag{8}$$

It is known from Eq. (8) that the peak value of the second-harmonic signal and concentration are linearly related; therefore, the gas concentration can be derived by measuring P_{2f}.

3. Experiment and Result Analysis

To verify the proposed method, the CH_4 absorption line at 1653.7 nm was used for the experiment to measure gas concentration from the reconstruction and fitting of second-harmonic signals.

Limited by the experimental conditions, we chose methane gas with a concentration of 5% to 30% for the experiment. In fact, by extending the path length through absorbing gas, the proposed method is suitable for the lower gas concentration detection. The key issues are the accuracy and stability of concentration measurements.

3.1. Experimental setup

The schematic diagram of the experimental system used in this investigation is shown in Fig. 1. A continuous-wavelength distributed-feedback tunable diode laser operating at 1653.7 nm and room temperature was used to measure the concentration of the CH_4. The required modulation signal is generated by an arbitrary function generator (UTG 1000A), which provides 5 Hz ramp wave and 5 kHz sine wave for wavelength scanning and harmonic detection, respectively. The laser beam was collimated by a 50 cm focal length lens. The interaction between the laser beam and the gaseous sample occurred in the sample cell.
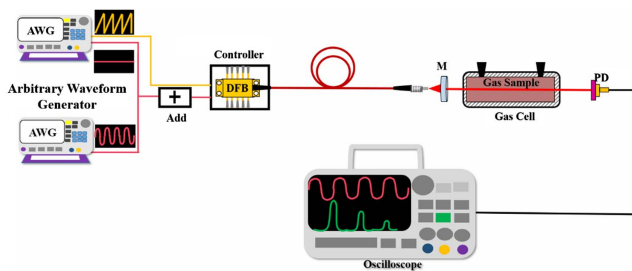

Fig. 1. Experimental setup for the validation of the proposed method.

Fixed gain amplified detectors (Thorlabs PDA20C) were used to record the signals obtained from the transmitted light. The photodiode signals used for the study were sent to the lock-in amplifier or acquired by using an oscilloscope (Keysight DSOX2012A) for FFT analysis. The data is subsequently forwarded to a computer to be processed.

The effectiveness of this method can be verified through two aspects. One is to verify whether the second-harmonic waveform reconstructed and fitted by FFT-WMS is consistent with the second-harmonic waveform directory extracted by WMS. The other is to compare the accuracy of the two measurements. The simulation diagram in Fig. 2 shows the main steps of two methods to extract the second-harmonic waveform. In WMS, the 5 Hz low-frequency ramp wave in Fig. 2(a) and the 5 kHz sine wave signal in Fig. 2(b) are superimposed to modulate the laser to form the incident light intensity in Fig. 2(c). The incident light intensity generates the transmission light intensity in Fig. 2(c) after passing through a certain concentration of gas cells, which is sent to the hardware lock-in amplifier (OE1022 SSI) to extract the second-harmonic waveform shown in Fig. 2(d). The inset of Fig. 2(c) that includes four peaks stands for light intensity at different wavelengths since the laser wavelength changes with the ramp wave.

In FFT-WMS, the incident light intensity in Fig. 2(f) is generated by the 5 kHz sine wave in Fig. 2(b) and the DC signal in Fig. 2(e). The second-harmonic value can be obtained by FFT analysis of the transmission light intensity under the DC signal. The second-harmonic waveform can be obtained by constantly changing the value of the DC signal and repeating the experiment, and the reconstructed second-harmonic waveform is shown in Fig. 2(g). The inset of Fig. 2(f) stands for a fixed wavelength since the laser operated at a fixed DC value.
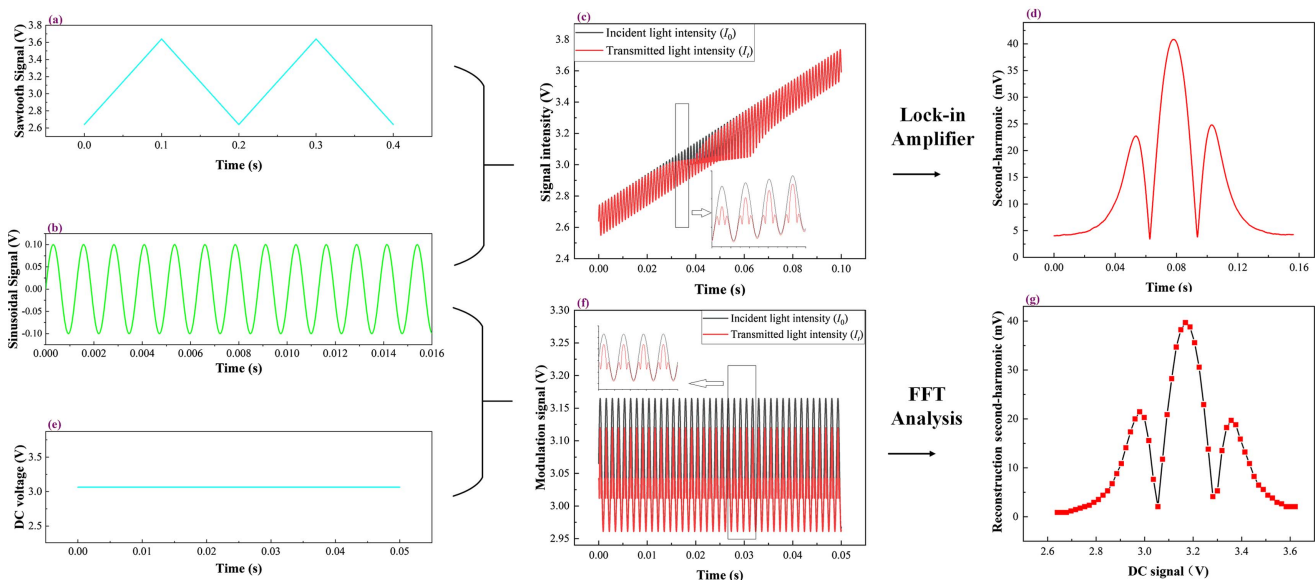

Fig. 2. (a)–(d) Represent the simulated process of extracting second harmonic using the WMS method. (b), (e)–(g) Represent the simulated process of extracting second harmonic using the FFT-WMS method.

3.2. Result and discussion

In our experiments, wavelength/intensity tuning of the diode laser was realized by changing the modulation signal. Among them, the amplitude of 5 kHz sine wave signal is 50 mV. In addition, a 5 Hz ramp wave signal (amplitude is 100 mV, offset is 440 mV, that is 390–490 mV) is used in WMS. A single experiment used a DC signal changing with intervals of 2 mV from 390 mV in FFT-WMS. Two experiments were repeated with 5%–30% CH_4 concentration. In the experiment, the other experimental conditions of the two methods are same.

Figure 3 shows the measured second-harmonic waveform results under atmospheric temperature and pressure by two means. The measurement results of both methods are in a high degree of consistency. This proves that the second-harmonic signal reconstructed and fitted by the FFT-WMS is consistent with the second-harmonic directory extracted by the WMS.

Table 1 is the comparison of concentration results measured by the WMS and FFT-WMS; the maximum concentration measurement errors for both are 4.50% and 2.87%, respectively. It can be seen from the table that the FFT-WMS generally has better measurement accuracy than the WMS method.

It can be seen from Eq. (8) that the peak value of the second-harmonic waveform has a linear relationship with the gas concentration. It can be seen from Fig. 4 that the peak value of the second-harmonic signal under FFT-WMS and gas concentration show a good linearity, and linear regression leads to regression coefficients $R^2 = 0.9993$. The relationship between them satisfies the formula $\chi_{CH_4} = 0.00495A + 0.00514$.

FFT-WMS remains essentially WMS. It does not use a low-frequency scanning signal. Therefore, FFT-WMS can avoid the effect of the low-frequency noise signal. In WMS, when a lock-in amplifier extracts each harmonic waveform, the low-frequency scanning signal (ramp wave) cannot be completely filtered out as noise, resulting in the distorted waveform of each harmonic, which affects the measurement result. In addition, the initial phase of the reference signal and the signal to be
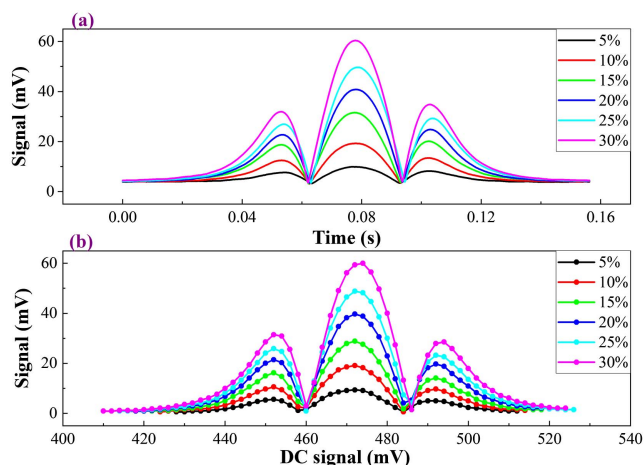
Table 1. Comparison of Concentration Results Measured by Two Methods.

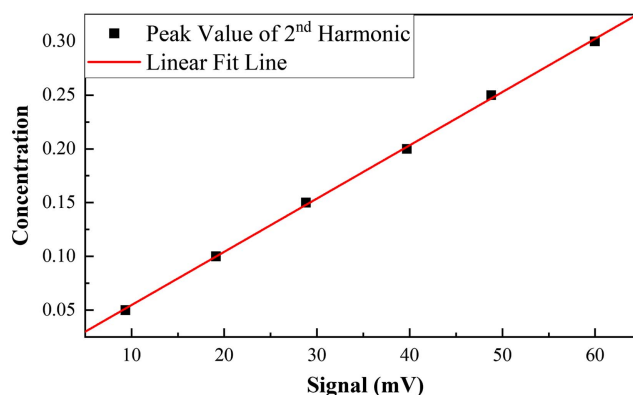| Conc (%)	FFT-WMS		WMS	
	Derived Conc (%)	Error (%)	Derived Conc (%)	Error (%)
5.00	5.14	2.87	4.94	−1.12
10.00	9.97	−0.27	9.58	−4.23
15.00	14.78	−1.49	15.68	4.50
20.00	20.16	0.80	20.25	1.24
25.00	24.67	−1.31	24.62	−1.52
30.00	30.20	0.67	29.94	−0.21

Fig. 4. Relationship between the peak value of the second-harmonic signal and the gas concentration under FFT-WMS.

measured will also affect the measured second harmonic. As with WMS, FFT-WMS is also affected by environmental factors (temperature, pressure), which can cause measurement errors. The RAM effect is also the main source of measurement error of the two methods.

Recently, researchers proposed and investigated the sparse Fourier transform (SFT)[15–18]. This is a discrete Fourier transform with less computational complexity than that of FFT. SFT can significantly accelerate the speed of spectrum analysis, which is helpful for applying FFT-WMS to the two-dimensional distribution detection of gas concentration in the future.

4. Conclusion

The principles and implementation of an alternative approach to obtain second-harmonic waveforms used for concentration calculation named FFT-WMS were described, and this method can improve the detection reliability and accuracy compared to WMS. The experiment of deriving gas concentration under different concentrations from 5% to 30% was carried out. Experiment results show that the second-harmonic waveform

Fig. 3. (a) Second-harmonic signal extracted from the lock-in amplifier using the WMS method. (b) Second-harmonic signal reconstructed by FFT-WMS.

reconstructed and fitted by the FFT-WMS is consistent with the second-harmonic waveform directory extracted by the WMS. Moreover, this method is less affected by low-frequency noise. The concentration error measured by the FFT-WMS is generally less than 3%, and the maximum error is only 2.87%. The resulting error measured by WMS under the same conditions is generally higher than that of FFT-WMS, and the maximum error is 4.5%.

In the WMS method, the price of the lock-in amplifier used to extract the second harmonic is expensive, whereas the FFT-WMS only needs the simple FFT analysis of the transmitted light intensity, and the cost is low. After determining the location of the absorption peak, the peak value of the second-harmonic waveform can be extracted for concentration measurement by a single FFT analysis, which significantly simplifies the experimental device and procedure. In the future, according to the above analysis, this method can also be extended to measure the gas concentration in computed tomography.

Acknowledgement

References

1. K. Krzempek, D. Tomaszewska, A. Foltynowicz, and S. Grzegorz, "Fiber-based optical frequency comb at 3.3 µm for broadband spectroscopy of hydrocarbons [Invited]," Chin. Opt. Lett. **19**, 081406 (2021).
2. K. W. Yang, H. L. Gong, X. L. Shen, Q. Hao, M. Yan, K. Huang, and H. P. Zeng, "Temperature measurement based on adaptive dual-comb absorption spectral detection," Chin. Opt. Lett. **18**, 051401 (2020).
3. X. Liu, J. B. Jeffries, R. K. Hanson, K. M. Hinckley, and M. A. Woodmansee, "Development of a tunable diode laser sensor for measurements of gas turbine exhaust temperature," Appl. Phys. B **82**, 469 (2006).
4. A. Farooq, J. B. Jeffries, and R. K. Hanson, "CO_2 concentration and temperature sensor for combustion gases using diode-laser absorption near 2.7 µm," Appl. Phys. B **90**, 619 (2008).
5. J. Li, Y. Du, Y. Ding, and Z. Peng, "Experimental and simulated study of line-shape models for measuring spectroscopic parameters using the WM-DAS method — part I: collisional broadening and absorption coefficients of H_2O-Ar system," J. Quant. Spectrosc. Radiat. Transf. **254**, 107216 (2020).
6. B. Li, C. Zheng, H. Liu, Q. He, W. Ye, Y. Zhang, J. Pan, and Y. Wang, "Development and measurement of a near-infrared CH_4 detection system using 1.654 µm wavelength-modulated diode laser and open reflective gas sensing probe," Sens. Actuat. B Chem. **225**, 188 (2016).
7. A. Upadhyay and A. L. Chakraborty, "Residual amplitude modulation method implemented at the phase quadrature frequency of a 1650 nm laser diode for line shape recovery of methane," IEEE Sens. J. **15**, 1153 (2015).
8. P. Dai, Y. Zhou, L. Wang, S. Liu, X. Zhang, and X. Chen, "Demodulation of the multi-peak fiber Bragg grating sensor based on partial wavelength scan," Chin. Opt. Lett. **18**, 071201 (2020).
9. Y. Du, Z. Peng, and Y. Ding, "Wavelength modulation spectroscopy for recovering absolute absorbance," Opt. Express **26**, 9263 (2018).
10. J. Reid and D. Labrie, "Second-harmonic detection with tunable diode lasers — comparison of experiment and theory," Appl. Phys. B **26**, 203 (1981).
11. L. Xu, N. Liu, S. Zhou, L. Zheng, B. Yu, H. Fischer, and J. Li, "Dual-frequency modulation quartz crystal tuning fork-enhanced laser spectroscopy," Opt. Express **28**, 5648 (2020).
12. D. Liu, N. Liu, S. Zhou, and J. Li, "Comparison of digital lock-in amplifier and fast Fourier transform algorithms for quartz-tuning-fork enhanced spectroscopy," Opt. Quantum Electron. **52**, 417 (2020).
13. S. Li and L. Sun, "Natural logarithm wavelength modulation spectroscopy," Chin. Opt. Lett. **19**, 031201 (2021).
14. R. Arndt, "Analytical line shapes for Lorentzian signals broadened by modulation," J. Appl. Phys. **36**, 2522 (1965).
15. A. C. Gilbert, M. J. Strauss, and J. A. Tropp, "A tutorial on fast Fourier sampling," IEEE Signal Process. Mag. **25**, 57 (2008).
16. S. Wang, V. M. Patel, and A. Petropulu, "Multidimensional sparse Fourier transform based on the Fourier projection-slice theorem," IEEE Trans. Signal Process. **67**, 54 (2019).
17. H. Zhang, T. Shan, S. Liu, and R. Tao, "Optimized sparse fractional Fourier transform: principle and performance analysis," Signal Process. **174**, 107646 (2020).
18. H. Zhang, T. Shan, S. Liu, and R. Tao, "Performance evaluation and parameter optimization of sparse Fourier transform," Signal Process. **179**, 107823 (2021).